J Geophys (1985) 57:90–105

Journal of Geophysics

Seismic modelling by methods of the theory of edge waves

K.D. Klem-Musatov and A.M. Aizenberg

Institute of Geology and Geophysics of the Siberian Branch of the Academy of Sciences of the USSR, Universitetskii prospekt 3. Novosibirsk, 90, USSR

Abstract. This paper deals with the computation of wavefields in 3-D inhomogeneous media containing structural elements such as pinch-outs, vertical and oblique contacts, faults, etc. The approach is based on the theory of edge waves. The total wavefield is considered as the superposition of two parts. The first part is described by the ray method. It has discontinuities because of its shadow boundaries. The second part is a superposition of two types of diffracted waves, caused by the edges and vertices of interfaces. This part smooths the above-mentioned discontinuities so that the total wavefield is continuous. Of special importance is the mathematical form of the amplitudes of diffracted waves, described with unified functions of eikonals. In fact, it allows all additional computations to be considered by finding the eikonals of diffracted waves. A modification of the ray method including diffraction by edges and vertices is described. A generalization of the concept of edge waves for caustic situations is given – the method of superposition of edge/tip waves. The result of such a generalization no longer supplements the geometrical seismic description, but completely replaces it by a new description valid for a broader class of wave phenomena (reflection/refraction, diffraction on edges and vertices, formation of caustics, etc.).

Key words: Diffraction on edges and vertices – Amplitudes of diffracted waves – Superposition of edge/tip waves

Introduction

The present article is an extended version of our report at the Workshop on Seismic Wave Propagation in Laterally Varying Media at Liblice, Czechoslovakia, 1983. Its main points were given in Klem-Musatov and Aizenberg (1984). Here we want to illustrate the main ideas of the theory of edge waves with the simplest examples and show how it is possible to use methods of this theory for seismic modelling.

Of special importance for seismology is the ray method which allows wavefields to be computed efficiently in 3-D inhomogeneous media far from the source (Babich and Alekseyev, 1958; Karal and Keller, 1959; Červený et al., 1977). However, the method gives only the components of the wavefields connected with the energy flux along the ray tubes but not diffusion through their side walls. If the main part of the wavefield is formed by diffusion, it cannot be described by the ray method. The desire to adapt this method to such situations has resulted in various modifications (Babich and Buldyrev, 1972; Popov, 1981; Červený, 1983; Kennett, 1984).

In the present paper a modification of the ray method for 3-D inhomogeneous block media is considered. The structural elements of interfaces in this type of media have sharp edges, the so-called diffracting edges (for example, the lines of pinch-outs, vertical and oblique contacts of interfaces, faults and so on). The ray method does not give a continuous description of the wavefields in this type of media because of shadow boundaries. The main idea of the present modification is to smooth the discontinuities by diffracted waves, scattered by the edges of interfaces, in such a way that the total wavefield is continuous. From a physical viewpoint, it is the same as adding the diffusion that is not considered by the ray method (Fock, 1965). This principle is well-known in the classical theory of diffraction (Born and Wolf, 1968) and in its modern modifications (Claerbout, 1976; Trorey, 1977; Hilterman, 1982; Fertig and Müller, 1979). However, there were no general formulae to use the above-mentioned idea for improving the ray method.

The very core of the present approach is connected with the so-called boundary layer approximation. It allows us to correct the results of the ray method only within the neighbourhood of the shadow boundaries. It is just this kind of approximation that makes the final formulae general and simple. The simplest way of getting these formulae is shown in this paper. It is based on assumptions concerning the analytical properties of the wavefields, but not the dynamic equations in any case. If a wave velocity is constant, the same formulae can be derived by the parabolic equation method or by an asymptotic analysis of the Kirchhoff integral. The formulae for the edge waves can be derived from a solution of the more general diffraction problem for wedge-shaped structures as well. For details on this subject, see Klem-Musatov (1980, 1981a, b) and Aizenberg (1982).

Offprint requests to: K.D. Klem-Musatov

Note that in the following monochromatic wavefields of angular frequency ω will be considered. The time factor $\exp(-i\omega t)$ with $i^2=-1$, where t is time, is omitted for convenience. Theoretical seismograms can also be computed in the time domain by the application of the Fourier transform.

Analytic results will be illustrated with theoretical seismograms. Two types of media are chosen for seismic modelling: a two-layered model and a three-layered one with a pinch-out. The top medium always has the following elastic parameters for both types of models: $\rho_1=2$ g/cm^3, $v_{P1}=2$ km/s, $v_{S1}=1.25$ km/s. The parameters of the bottom are always $\rho_2=2.4$ g/cm^3, $v_{P2}=2.5$ km/s, $v_{S2}=1.5$ km/s. Parameters of the pinched layer are $\rho_3=1.8$ c/cm^3, $v_{P3}=1.75$ km/s, $v_{S3}=1.05$ km/s. The observation system is located in the top medium. It contains either a profile of observation points (they are marked by circles in the figures) and a single source of oscillations (it is marked by an asterisk), or a profile of matched sources with observation points (they are marked by crosses). The source of oscillations excites a P wave with a spherical directivity pattern. The shape of the radiated pulse is $f(t)=t\exp(-\beta t)\sin(2\pi t/T)$, where t is time, $0\leqq t\leqq 4T$, $\beta=50$ Hz, $T=0.03$ s. On changing to the nonstationary case the Hilbert transformation for narrow-band signals was used. All components of a displacement vector of seismic waves can be computed. In numerical examples (except Fig. 23) we show only the Z-component of PP waves. The X-component is oriented along a profile, the Z-component is oriented upwards. All metrical values are given in kilometres, as time is given in seconds.

Ray method

First of all, let us recollect the basic principles of the ray method. The model of the medium is considered as a combination of domains and interfaces. The functions, describing physical properties within the domains, are continuous and slowly changing. A surface formed by points of discontinuity of any of these functions is called an *interface*. A point of the interface is considered as *regular* if the surface is continuous together with its first and second tangential derivatives. A part of the interface is considered as *regular* if its points are all regular. The ray method allows us to describe only those components of the wavefield that are connected with reflections/transmissions at the regular parts of interfaces. The description has the form of superposition of the single waves

$$f=\sum_m f_m. \tag{1}$$

Let us give the main definitions related to a single wave f_m.

Kinematics

A ray is a space curve, the tangential unit vector $\mathbf{e}_m$ of which complies with the differential equation:

$$\frac{\mathrm{d}}{\mathrm{d}s}(\mathbf{e}_m/v_m)=\operatorname{grad}(1/v_m) \tag{2}$$

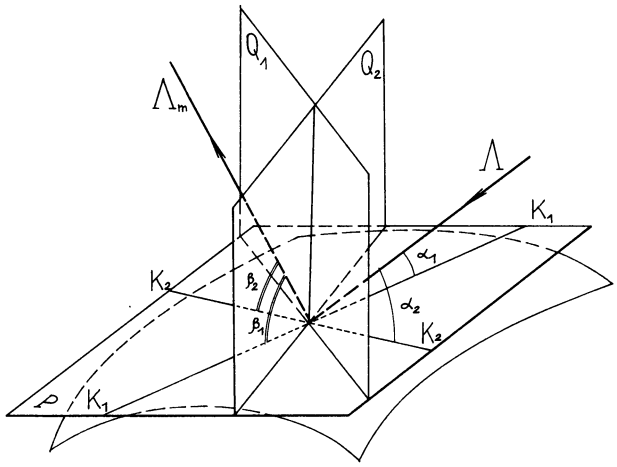

Fig. 1. Interpretation of Snell's law. Explanation in text

where ds is the differential of the arc length and v_m is the wave velocity. This equation determines the ray uniquely if its initial direction is given, and if a connection between the directions of incident and reflected/transmitted rays at the points of the interfaces is also given. The latter is expressed by Snell's law. In this law the geometry of the interface is usually characterized by the position of the normal to the interface. However, in this paper it is more convenient to achieve this by means of a tangential plane to the interface.

Let K_1 and K_2 be tangents to two arbitrary intersecting curves of the interface at the point of incidence (Fig. 1). As a results we get the position of the tangential plane P at any regular point of interface. Let α_1 and α_2 be acute angles between the incident ray Λ and the lines K_1 and K_2, respectively. Let β_1 and β_2 be acute angles between the reflected/transmitted ray Λ_m and the same lines K_1 and K_2. Let Q_1 and Q_2 be the planes that are normal to the lines K_1 and K_2 at the point of incidence. Then Snell's law can be expressed in the following way (Klem-Musatov, 1980):

1) The incident and the secondary ray lie on different sides of the planes Q_1 and Q_2,

2) The directions of the above rays comply with the conditions:

$$\cos\beta_1/v_m=\cos\alpha_1/v, \qquad \cos\beta_2/v_m=\cos\alpha_2/v \tag{3}$$

where v and v_m are the velocities of the incident and reflected/transmitted wave, respectively.

Dynamics

If a set of rays $\mathbf{e}_m$ is a two-parameter set of space curves, it is called *a congruence* (Born and Wolf, 1968). A single wave

$$f_m=\Phi_m\exp(i\omega\tau_m) \tag{4}$$

is connected with a congruence of the rays $\mathbf{e}_m$. Its eikonal τ_m complies with the differential equation:

$$\operatorname{grad}\tau_m=\mathbf{e}_m/v_m. \tag{5}$$

Equation (4) itself may represent a scalar wave (optics, acoustics) or a vector wave (elastodynamics, electrodynamics). In the first case, the ray amplitude Φ_m is a scalar one. In the second case,

$$\Phi_m = \mathbf{p}_m \varphi_m \tag{6}$$

where $\mathbf{p}_m$ is a unit vector of polarization, and φ_m is a scalar. In an isotropic medium the vector $\mathbf{p}_m$ coincides with the vector $\mathbf{e}_m$ (a longitudinal wave) or is perpendicular to $\mathbf{e}_m$ (a transverse wave).

The scalar amplitude Φ_m (or φ_m) complies with the so-called transport equation

$$2 \operatorname{grad} \tau_m \cdot \operatorname{grad} \Phi_m + B_m \Phi_m = 0 \tag{7}$$

where the coefficient B_m depends on the kind of original accurate equations of optics, accoustics (or elastodynamics, electrodynamics). The solution of Eq. (7) is well known:

$$\Phi_m = \kappa_m L_m^{-1/2}, \qquad L_m = \exp\left(\int_0^{\tau_m} v_m^2 B_m \, \mathrm{d}\tau_m\right) \tag{8}$$

where integration must be performed along the ray. The choice of the constant κ_m must comply with the boundary conditions. In fact, κ_m is the product of reflection/transmission coefficients of plane waves. Only the first term of the ray series is shown. As will be seen later, the subsequent approach does not deal with the explicit formulae for the ray amplitude Φ_m.

Edge waves

We extend the theoretical basis using the ideas of the theory of diffraction. Let a certain line be formed by points of discontinuity of an interface or any of its first or second tangential derivatives. It is a common linear element of the regular parts of a single interface or of several interfaces. This type of line is called *an edge*. A point of the edge is considered *regular*, if the corresponding line is continuous together with its first tangential derivative. The edge is considered *smooth* if its points are all regular.

Every single wavefield f_m exists within a connected domain of continuity. This domain is called *the primary illuminated zone*. If the interfaces have edges, there may be a domain in which the wave f_m does not exist (we define it as $f_m \equiv 0$). This type of domain is called *the primary shadow zone* of the wave. The singlyconnected surface dividing these zones is called *the primary shadow boundary*. Let mn be the double number of each primary shadow boundary of the wave f_m. Let Ω_{mn}^+ be a symbol of the primary shadow zone, formed by the mn-th shadow boundary. Let Ω_{mn}^- be the symbol of the primary illuminated zone. The non-caustic shadow boundaries formed by the edges are considered.

Figure 2 shows the simplest example of the above definitions for a wave reflected from a half-plane. Let us mark this wave by $m=1$, and its shadow boundary by $m=1$, $n=1$. Figure 3a shows the reflected wave. The primary illuminated zone Ω_{11}^- is $x \leqq 1.15$ km, the primary shadow zone Ω_{11}^+ is $x > 1.15$ km.

We can see that shortcomings of Eq. (1) appear as discontinuities of the wavefields f_m at the primary shadow boundaries. Let us see how this can be corrected.

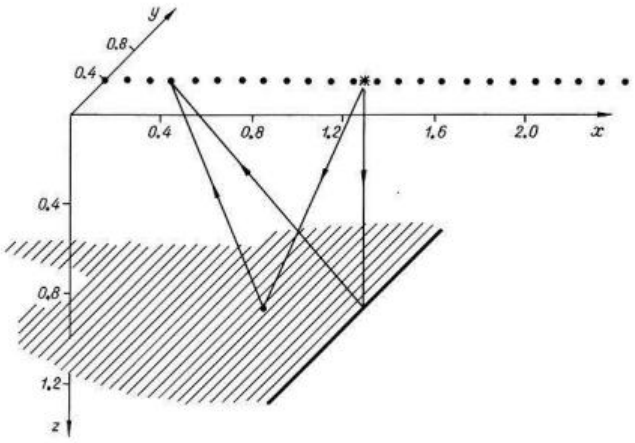

Fig. 2. Model of "half-plane". Reflecting interface coincides with shaded region

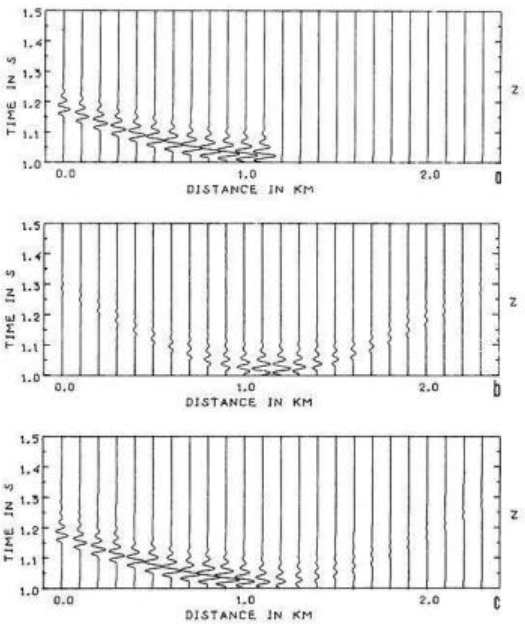

Fig. 3a–c. Theoretical seismograms for model of "half-plane": **a** reflected wave, **b** edge wave (twice enlarged), **c** total field

Kinematics

We use a formal method to find the directions of the rays, generated at the points of an edge. Let the ray impinge on any regular point of the edge. The direction of a secondary ray must comply with Snell's law, Eq. (3). It is necessary to fix the positions of the pair of lines K_1 and K_2, i.e. to set the position of the plane P. One of the two lines (for example, K_1) must be the tangent to the edge because it is a common linear element of the interfaces (Fig. 4). However, there are no limitations in choosing the direction of the second line K_2. That is why any plane, containing the tangent to the edge, may be considered as plane P. Let incident Λ and secondary Λ_{mn} rays make the acute angles α and β,

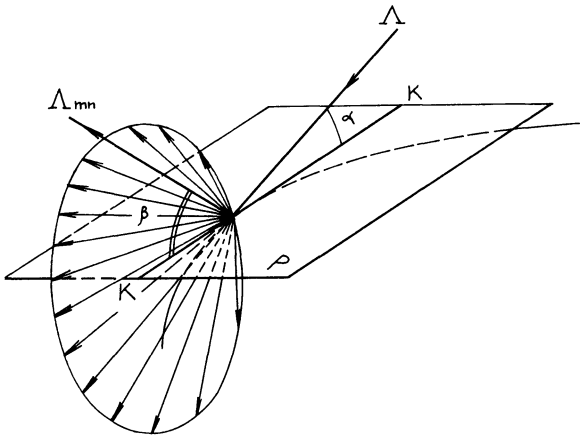

Fig. 4. A cone of diffracted rays. Explanation in text

respectively, with the tangent to the edge. Then Snell's law appears in the following form:

$$\cos\beta/v_m = \cos\alpha/v. \tag{9}$$

Note, the one-parameter set of secondary rays complies with this condition.

The above-mentioned fact is known as *the law of edge diffraction* (Keller, 1962). It reads as follows. Let an incident ray make an acute angle α with the tangent to an edge. The set of secondary rays forms a cone with its vertex at the point of incidence. Its apex angle is 2β, where β and α are connected under Eq. (9). The incident ray and the above-mentioned cone lie on opposite sides of the plane normal to the edge at the point of incidence. Obviously, this law holds true within a small neighbourhood of the point of incidence, in which it is possible to neglect the curvature of the rays.

Take $\mathbf{e}_{mn}$ to be the unit vector of the tangent to the ray. Let this ray comply with Eq. (9) for that edge, which gives the mn-th primary shadow boundary. Then the differential equation:

$$\frac{d}{ds}(\mathbf{e}_{mn}/v_m) = \operatorname{grad}(1/v_m) \tag{10}$$

determines the congruence of *the edge diffracted rays.*

An edge diffraction coefficient

Let the wave

$$f_{mn} = \Phi_{mn}\exp(i\omega\tau_{mn}), \qquad \operatorname{grad}\tau_{mn} = \mathbf{e}_{mn}/v_m \tag{11}$$

be connected with the mn-th primary shadow boundary. The latter may be given implicitly by the equation $\tau_{mn} = \tau_m$. For example, in Fig. 2 such a boundary is given by the relation $x = 1.15$ km. The wave, Eq. (11), is called *an edge-diffracted wave.* Now we have come to the description of diffracted waves.

Let τ_{mn}, η, ζ be the ray coordinates of the wave f_{mn}. Here η and ζ give a congruence of the diffracted rays, i.e. every pair of fixed values $\eta = constant$ and $\zeta = constant$ gives a single ray. This pair of coordinates may be chosen in many different ways. Let the coordinate surface $\eta = 0$ coincide with the mn-th primary shadow boundary $\tau_{mn} = \tau_m$, so that the primary shadow zone of the wave f_m coincides with the domain $\eta > 0$. The coordinate surfaces $\zeta = constant$ may be taken arbitrarily.

In the first place, let us take the case when the amplitude Φ_m of the wave, Eq. (4), is a scalar one. Generalization of the present approach for polarized waves will be given in a following section. However, it is more convenient to use numerical examples for polarized waves before the mentioned generalization.

Let the wave, Eq. (4), be a function of the above-mentioned ray coordinates

$$f_m = \Phi_m(\tau_{mn}, \eta, \zeta)\exp[i\omega\tau_m(\tau_{mn}, \eta, \zeta)]. \tag{12}$$

Then this wavefield in the neighbourhood of its shadow boundary may be represented by the discontinuous function:

$$f_m = f_m(\tau_{mn}, \eta, \zeta) \quad \text{when } \eta < 0,$$
$$f_m = 0 \quad \text{when } \eta > 0 \tag{13}$$

which displays explicitly the shortcomings of the ray method.

Suppose, Eq. (13) represents an analytic function of the variable η and allows us to make an analytic continuation into the complex plane of η for any permissible values τ_{mn} and ζ. Let us find f_{mn} among the piecewise-analytical functions descreasing at infinity ($f_{mn} \to 0$, when $|\eta| \to \infty$). Then we may construct the following integral of Cauchy's type

$$f_{mn} = \frac{1}{2\pi i}\int_L f_m(\tau_{mn}, \eta + \alpha, \zeta)\frac{d\alpha}{\alpha} \tag{14}$$

where L is some smooth infinite contour of integration. The specific type of this contour will be given in the following.

The integral in Eq. (14) has the following properties. It is zero when $|\eta| \to \infty$. It has a discontinuity when $\eta = 0$. However, the superposition of Eqs. (13) and (14) is a continuous and analytic function of η within the neighbourhood of the surface $\eta = 0$. If the function (13) is a solution of some linear differential equation (for example, the wave equation) within the domain $\eta < 0$, then the superposition of Eqs. (13) and (14) complies with the same equation for $\eta < 0$ as well as for $\eta > 0$.

When $\omega \to \infty$, the asymptotic value of integral (14) can be found by *the method of canonical integrals* (Felsen and Marcuvitz, 1973). Since this value is formed by contributions within a small neighbourhood of the saddle point $\alpha = -\eta$, let us take the standard approximations at this point

$$\Phi_m \approx \Phi_m(\tau_{mn}, 0, \zeta),$$
$$\tau_m \approx \tau_m(\tau_{mn}, 0, \zeta) + \eta^2/2\left(\frac{\partial^2\tau_m}{\partial\eta^2}\right)_{\eta=0} \tag{15}$$

and use the following relations:

$$\tau_m(\tau_{mn}, 0, \zeta) = \tau_{mn}, \qquad \left(\frac{\partial^2\tau_m}{\partial\eta^2}\right)_{\eta=0} \approx \frac{2}{\eta^2}(\tau_m - \tau_{mn}). \tag{16}$$

Let the contour L within a neighbourhood of the saddle point coincide with *the steepest descent path*

$$\mathrm{Im}[i\omega\tau_m(\tau_{mn}, \eta+\alpha, \zeta)] = \mathrm{Im}[i\omega\tau_m(\tau_{mn}, 0, \zeta)],$$

$$\mathrm{Re}[i\omega\tau_m(\tau_{mn}, \eta+\alpha, \zeta)] < 0.$$

Using τ_m from Eq. (15) gives the following equations for this part of the contour

$$\mathrm{Re}\,\alpha+\eta = -\mathrm{Im}\,\alpha \quad \text{for } \tau_{mn} > \tau_m,$$

$$\mathrm{Re}\,\alpha+\eta = \mathrm{Im}\,\alpha \quad \text{for } \tau_{mn} < \tau_m.$$

The integral exists, if the contour approaches the points $\mathrm{Im}\,\alpha = \pm\infty$ within domains $\mathrm{Re}[i\omega\tau_m(\tau_{mn}, \eta+\alpha, \zeta)] < 0$. Using τ_m from Eq. (15) allows us to obtain this condition for $\mathrm{Im}\,\alpha \to \infty$ in the following form

$$-\pi < \mathrm{Re}\,\alpha+\eta < 0 \quad \text{when } \tau_{mn} > \tau_m,$$

$$0 < \mathrm{Re}\,\alpha+\eta < \pi \quad \text{when } \tau_{mn} < \tau_m,$$

and for $\mathrm{Im}\,\alpha \to -\infty$ in the form

$$0 < \mathrm{Re}\,\alpha+\eta < \pi \quad \text{when } \tau_{mn} > \tau_m,$$

$$-\pi < \mathrm{Re}\,\alpha+\eta < 0 \quad \text{when } \tau_{mn} < \tau_m.$$

The contours are shown in Fig. 5a for $\tau_{mn} > \tau_m$ and in Fig. 5b for $\tau_{mn} < \tau_m$ (in these figures $q=1$).

Then integral (14) may be written as

$$f_{mn} = s_{mn}\Phi_m W(w_{mn}) \exp(i\omega\tau_{mn}),$$

$$w_{mn} = \sqrt{2\omega(\tau_{mn}-\tau_m)/\pi}, \tag{17}$$

$$s_{mn} = +1 \quad \text{within } \Omega^+_{mn}, \quad s_{mn} = -1 \quad \text{within } \Omega^-_{mn},$$

$$W(w) = \exp(-i\pi w^2/2)/(2\sqrt{\pi}) \int_{-i\pi w^2/2}^{\infty} t^{-1/2}\exp(-t)\,dt \tag{18}$$

where W may be regarded as *an edge diffraction coefficient*. If $\tau_{mn} < \tau_m$, we have $w_{mn} = ix$, $x = \sqrt{2\omega(\tau_m-\tau_{mn})/\pi}$, $W(ix) = \overline{W}(x)$, where $\overline{W}$ denotes the complex conjugate of W. In these formulae we may use the analytic continuation of the amplitude Φ_m and the eikonal τ_m into the primary shadow zone by means of any type of parametrization of space.

Figure 3b shows the edge wave computed by Eq. (17).

Note, that the function $W(w)$ can be represented by known special functions

$$W(w) = (2\sqrt{\pi})^{-1}\Psi(1/2, 1/2; z) = (2\sqrt{\pi})^{-1}\exp(z)\Gamma(1/2, z),$$

$$z = -i\pi w^2/2 \tag{19}$$

where $\Psi(1/2, 1/2; z)$ is a confluent hypergeometric function, and $\Gamma(1/2, z)$ is an incomplete gamma function.

If $0 \leqq w < \infty$, we have the following approximate formulae:

$$W(w) = W(0) + w/\sqrt{2}\cdot\exp(i3\pi/4) + O(w^2),$$

$$W(0) = 1/2 \quad \text{when } w \to 0, \tag{20}$$

$$W(w) = \exp(i\pi/4)/(\sqrt{2}\pi w) + O(w^{-2}) \quad \text{when } w \to \infty$$

where O is the symbol of asymptotic estimation. Figure 6 shows the graph of the function $W(w)$, Eq. (18).

Now we shall briefly discuss the type of approximation given by Eq. (17). Obviously, the above approach is approximate even in a high-frequency sense, because of the disturbance of the boundary conditions at interfaces by the integral (14). To be more accurate, it would be necessary to add a certain term δf_{mn} to the integral (14) to satisfy the boundary conditions. In principle, this term can be found by using the geometrical theory of diffraction (for example, see Klem-Musatov (1980) for the case $v_m = \text{constant}$). It is essential that such an addition δf_{mn} would have no discontinuity at the primary shadow boundary $\eta = 0$. Using the geometrical theory of diffraction (Klem-Musatov, 1980) allows us to estimate the value to the order of $\delta f_{mn} \sim O(\omega^{-1/2})$ except for grazing and critical regions.

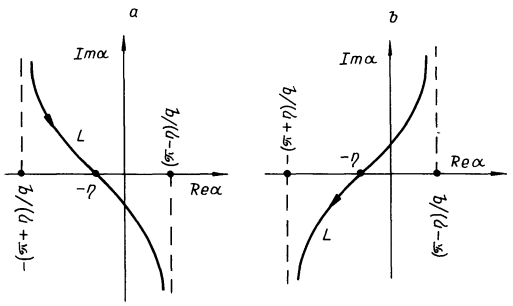

Fig. 5a and b. The contours of integration. Explanation in text

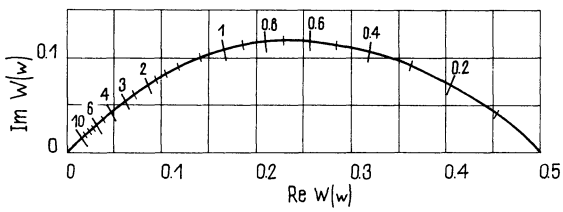

Fig. 6. Function $W(w)$ of the real variable w. Numbers above the curve give the values of w

Let us see how it would be connected with Eq. (17). According to Eq. (20), the amplitude of the edge wave changes its value from an asymptotic estimation $O(1)$ at $w_{mn} = 0$ to $O(\omega^{-1/2})$ at $w_{mn} \to \infty$. The gradient of this function depends on w_{mn}. Let us write w_{mn} in the form

$$w_{mn} = \sqrt{2N}, \quad N = v_m(\tau_{mn}-\tau_m)/(\lambda/2), \quad \lambda = 2\pi v_m/\omega$$

where N presents the phase difference in the half-period Fresnel zones. If $N = 0, 1, 2, 3, 4, 5, \ldots$ we have, respectively, $|W| = 0.50;\ 0.17;\ 0.11;\ 0.09;\ 0.08;\ 0.07; \ldots$. We can see that this function changes rapidly when $N < 2 (w_{mn} < 2)$ and slowly when $N > 2$. By the way, the second part ($w_{mn} \to \infty$) of Eq. (20) is true for $w_{mn} > 2$. The domain of this rapid change forms a neighbourhood of the primary shadow boundary. It is called *a boundary layer*, with a position determined by the inequality $w_{mn} \lesssim 2$. Within the boundary layer an inaccuracy $\delta f_{mn} \sim O(\omega^{-1/2})$ of Eq. (17) may be considered of no importance in comparison with $O(1)$. In Fig. 3 the boundary layer occupies a domain $0.85\ \mathrm{km} \lesssim x \lesssim 1.45\ \mathrm{km}$. Outside the boundary layer the amplitude of the edge wave has the same asymptotic

estimation $O(\omega^{-1/2})$ as δf_{mn}. It is clear that Eq. (17) fails here. More accurate analysis of the integral (14) would not improve the properties of this formula. Thus, Eq. (17) gives a satisfactory result only within the boundary layer. All this is quite enough for correcting the ray method.

Figure 3c shows the total wavefield $f=f_1+f_{11}$ formed by the superposition of reflected f_1 and edge f_{11} waves.

Equation (17) has one other local property, which allows us to interpret the forthcoming results. According to Eq. (15), a value of Φ_m would be taken at the primary shadow boundary $\Phi_m=\Phi_m(\tau_{mn},0,\zeta)$. However, it is possible to consider Φ_m as a function of the free point $\Phi_m=\Phi_m(\tau_{mn},\eta,\zeta)$ as well because the difference $\Phi_m(\tau_{mn},\eta,\zeta)-\Phi_m(\tau_{mn},0,\zeta)$ is so small in comparison with Φ_m within the boundary layer. The real accuracy of the description of the edge wave is independent of the choice of the above versions. By the way, this is the reason why Φ_m may be continued analytically into the shadow zones.

Interrelation with known physical ideas

We consider briefly, how the above theory matches the concept of Fresnel-Kirchhoff's *secondary sources* and Fock's concept of *transverse diffusion.*

Using Eq. (19) we can represent the superposition of reflected waves, Eq. (13), and edge waves, Eq. (17), within a boundary layer in the form

$$f_m+f_{mn}=f_m\mathrm{F}(-s_{mn}w_{mn}\sqrt{\pi/2}), \tag{21}$$

$$\mathrm{F}(z)=\pi^{-1/2}\exp(-i\pi/4)\int_{-\infty}^{z}\exp(ix^2)\,\mathrm{d}x$$

where $\mathrm{F}(z)$ is the Fresnel integral. If the wave velocity is constant, the same formula can be derived by an asymptotic analysis of the Kirchhoff integral (Klem-Musatov, 1980; Aizenberg, 1982). Thus Eq. (17) matches the classical ideas of Fresnel-Kirchhoff's theory of diffraction.

Let us show with the simplest example that Eq. (17) also complies with the so-called Fock's parabolic equation of *transverse one-dimensional diffusion* which describes diffusion of the wave energy out of the primary illuminated zone into the primary shadow zone. Let the wave velocity be constant and the wave f_m be plane ($\Phi_m=constant$) with its wave vector perpendicular to an edge. Let (r,θ,z) be the cylindrical ray coordinates, where r is the distance along a diffracted ray from the edge, θ is the angle between the diffracted ray and the shadow boundary $\theta=0$, z is the distance along the edge. By substitution of Eq. (17) into Helmholtz's equation $(\Delta+k_m^2)f_{mn}=0$, where $k_m=\omega/v_m$, and neglecting all values within an order less than k_m, we can obtain the well-known equation of transverse diffusion

$$\frac{2ik_m}{\sqrt{r}}\frac{\partial}{\partial r}(\sqrt{r}\,\Phi_{mn})+\frac{1}{r^2}\frac{\partial^2}{\partial\theta^2}\Phi_{mn}=0. \tag{22}$$

Using the following relations within a boundary layer,

$$w_{mn}=\sqrt{2\omega(\tau_{mn}-\tau_m)/\pi}=\sqrt{2k_mr(1-\cos\theta)/\pi}\approx\theta\sqrt{k_mr/\pi},$$

we can represent Eq. (22) in the form

$$z\frac{\mathrm{d}^2}{\mathrm{d}z^2}\Phi_{mn}+(1/2-z)\frac{\mathrm{d}}{\mathrm{d}z}\Phi_{mn}-1/2\,\Phi_{mn}=0,$$

$$z=-i\pi w_{mn}^2/2. \tag{23}$$

The solution of this equation is function $W(w)$ in Eq. (19). Thus Eq. (17) describes the phenomenon of transverse diffusion in the form of the edge wave. An analysis shows the following mechanism of this phenomenon. The wave energy flows from the primary illuminated zone through the shadow boundary into the shadow zone along a cone of diffracted rays. There is no energy exchange between neighbouring cones (Klem-Musatov, 1980).

Note, if the wave velocity is constant, Eq. (17) is a first approximation of the more precise description of the edge wave by the successive approximation method in the form of an infinite series (Klem-Musatov, 1980).

Polarization

Now let us take the case when the amplitude of wave (4) is the vector (6). Let $\mathbf{j}_1$, $\mathbf{j}_2$, $\mathbf{j}_3$ be the unit vectors of a certain fixed coordinate system (for example, the Cartesian one). Let us decompose the vector (6) on the above basis and represent the wave (4) in the form

$$f_m=\mathbf{p}_m\varphi_m\exp(i\omega\tau_m)=\sum_{q=1}^{3}\mathbf{j}_q f_m^{(q)},$$

$$f_m^{(q)}=\varphi_m^{(q)}\exp(i\omega\tau_m) \tag{24}$$

where the $f_m^{(q)}$ are scalars. We represent the edge wave, Eq. (11), on the same basis:

$$f_{mn}=\sum_{q=1}^{3}\mathbf{j}_q f_{mn}^{(q)},\qquad f_{mn}^{(q)}=\varphi_{mn}^{(q)}\exp(i\omega\tau_{mn}) \tag{25}$$

where the $f_{mn}^{(q)}$ are scalars. We use the same approach, Eqs. (12)–(17), for every scalar function $f_m^{(q)}(\tau_{mn},\eta,\zeta)$ which was used for function (12). It allows us to determine three scalar functions:

$$f_{mn}^{(q)}=s_{mn}\varphi_m^{(q)}W(w_{mn})\exp(i\omega\tau_{mn})\quad\text{with}\quad q=1,2,3. \tag{26}$$

Inserting Eq. (26) into Eq. (25) gives, once again, Eq. (17), where Φ_m is the vector (6).

This result has to be interpreted. Let $\mathbf{p}_{mn}$ be a unit vector of polarization of the edge wave f_{mn}. In accordance with the general theory this vector must coincide with $\mathbf{e}_{mn}$ (a longitudinal wave) or be perpendicular to $\mathbf{e}_{mn}$ (a transverse wave). But in Eq. (17) the vector $\mathbf{p}_{mn}$ coincides with $\mathbf{p}_m(\tau_{mn},0,\zeta)$ which is out of the line of general theory. In other words, the above approach gives an inaccuracy $\delta\mathbf{p}=\mathbf{p}_{mn}(\tau_{mn},\eta,\zeta)-\mathbf{p}_m(\tau_{mn},0,\zeta)$. In fact, the real accuracy of the description of polarization is independent of the choice of any of the versions: $\mathbf{p}_m(\tau_{mn},0,\zeta)$, $\mathbf{p}_m(\tau_{mn},\eta,\zeta)$ or $\mathbf{p}_{mn}(\tau_{mn},\eta,\zeta)$ because the corresponding $\delta\mathbf{p}$ is of no importance in comparison with $\mathbf{p}_{mn}$ within the boundary layer. That is why the vector Φ_m may be considered a function of the free point $\Phi_m(\tau_{mn},\eta,\zeta)$ and then continued analytically into the shadow zones.

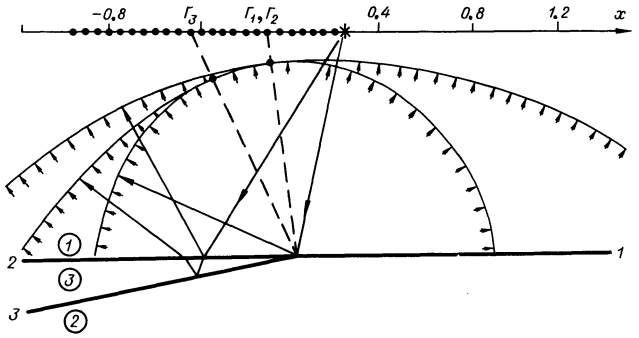

Fig. 7. Model of "pinch-out" and wavefronts in cross-section with projection of the observation system. The profile of observation is perpendicular to the edge. The angle of the pinch-out is 5°

Ray method with consideration of edge diffraction

The present modification of the ray method results in the addition of edge waves, Eq. (17), to the reflected/transmitted wavefield, Eq. (4)

$$f=\sum_m(f_m+\sum_n f_{mn}).$$

This approach can be used outside caustic zones in any inhomogeneous medium with smooth edges of interfaces.

Here we shall show an example of using this approach for the model of a pinch-out (Fig. 7). Inside the pinched layer there are multiple reflections. As a result, there are many reflected waves with sharp shadow boundaries at the profile of observation. Only three of them are shown in Fig. 7. Let us mark them by $m=1,2,3$. We mark their shadow boundaries by $m1$. They are shown with dashed lines (Γ_1,Γ_2 relating to interfaces 1 and 2, and Γ_3 to interfaces 3 with PP-transmission through interface 2). The total wavefield is $f=\sum_m^3(f_m+f_{m1})$. Figure 8 shows the wavefields. Note that all edge waves from the common edge have the same eikonal and form a total diffracted wave. One can see that the addition of edge waves essentially changes the wavefield compared with the ray method wavefield.

The method of superposition of edge waves

Equations (4) and (17) allow us to compute wavefields in 3-D inhomogeneous media with smooth edges of interfaces outside caustic zones. There is an approach, based on the above formulae, which can also be used within the caustic zones if they are formed by the curvature of interfaces (Aizenberg and Klem-Musatov, 1980). Let us describe the idea in brief. The wavefield scattered by a rectifiable interface can be replaced approximately by the field scattered by a piecewise-plane boundary, which is approximated by a sufficiently large number of plane elements.

This approximation guarantees finite values of the terms Φ_m in Eqs. (4) and (17) because they now do not depend on the curvature of the initial interface. The wavefield scattered by the piecewise-plane boundary is

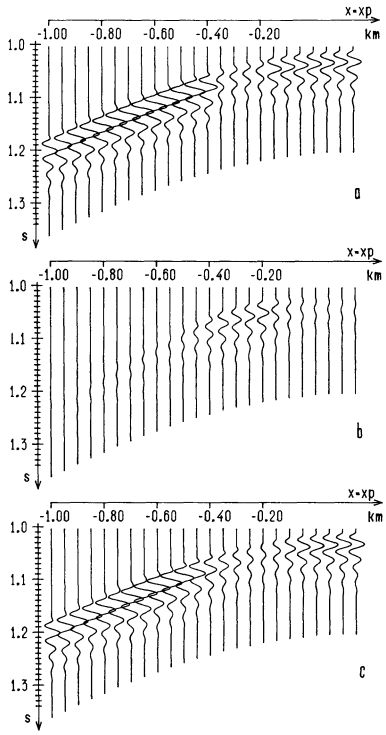

Fig. 8a–c. Theoretical seismograms for model of "pinch-out": **a** reflected waves, **b** edge waves, **c** total field

the superposition of fields scattered by the plane elements composing it.

The simplest version of this approach occurs when the original interface is a cylindrical surface and only single scattering is taken into consideration. Then each element of the piecewise-plane boundary is an infinite band with two rectilinear edges. For a sufficiently small step of approximation, the contributions from the elements, containing reflection/transmission points, are small enough and may be neglected. Then the field scattered by an individual plane element will be the superposition of two edge waves diverging from its edges. The total field can be represented by superposition of just edge waves alone

$$f=\sum_{m=1}^{M}\Delta f_m,\qquad \Delta f_m=\sum_{n=1}^{2}f_{mn},\qquad m\neq m_0 \tag{27}$$

where m coincides with the index of an element, n coincides with the index of an edge, m_0 are the indices of elements containing reflection/transmission points.

To justify the above approach, we will take Eq. (27) to the limit of the initial interface, simultaneously letting the step of approximation tend to zero and increasing the number of elements. In this case

$$\lim_{\substack{\max\{\Delta l_m\}\to 0\\ M\to\infty}}\sum_{m=1}^{M}\Delta l_m=\int_L \mathrm{d}l, \tag{28}$$

$$f=\int_L F(l)\exp[i\omega\tau(l)]\,\mathrm{d}l,$$

$$F(l)=\Phi_0(l)[-i\omega/(4\pi)]^{1/2}\left|\frac{\partial\tau}{\partial l}\right|(\tau-\tau_0)^{-1/2}$$

where $\Phi_0(l)$ and τ_0 are the amplitude and the eikonal of the analytic reflection/transmission for point l, and τ is the eikonal of the scattered wave. Here the analytic reflection/transmission stands for the usual reflection/transmission from/through the plane boundary which is a tangent to the initial interface at point l.

Equation (28) can be regarded as a new asymptotic formulation of *the concept of secondary sources*. According to this formulation the value of the field at any point of the medium will be the superposition of secondary waves with amplitude $F(l)\,dl$ diverging from each point of the initial interface. Analysis shows that, unlike the classical Fresnel and Kirchhoff descriptions, the amplitudes of the secondary waves in Eq. (28) are strictly bounded on the contour of integration.

Within the concept of secondary sources obtained we can explain the phenomena of regular reflection/transmission of waves, formation of caustics, edge effects and the phenomena of scattering of waves by interfaces of complex form. It is known that the asymptotic behaviour of integrals of the type in Eq. (28), for large values of ω, is determined by stationary points of the function $\tau(l)$, singular points for the function $F(l)$ and the end points of the contour of integration (Felsen and Marcuvitz, 1973). The asymptotic analysis in the neighbourhood of an isolated stationary point of the first order gives the wavefield, Eq. (28), in the form of a regular wave

$$f=\Phi(l_1)\exp[i\omega\tau(l_1)], \tag{29}$$

$$\Phi(l_1)=\Phi_0(l_1)\left[1-\frac{\partial^2\tau_0(l_1)}{\partial l^2}\Big/\frac{\partial^2\tau(l_1)}{\partial l^2}\right]^{-1/2}.$$

If the wave velocity is constant, this formula coincides with the formula of the ray method.

The asymptotic analysis of integral (28) in the neighbourhood of an isolated stationary point of second order gives the approximation for a simple caustic

$$f=\Phi(l_2)\,\mathrm{Ai}(q)\exp[i\omega\tau(l_2)],$$

$$\Phi(l_2)=\Phi_0(l_2)(-i\pi/\omega)^{1/2}|q|[\tau(l_2)-\tau_0(l_2)]^{-1/2}, \tag{30}$$

$$q=\omega^{2/3}2^{1/3}\frac{\partial\tau(l_2)}{\partial l}\left[\frac{\partial^3\tau(l_2)}{\partial l^3}\right]^{-1/3}$$

where $\mathrm{Ai}(q)$ is the Airy function. The same analysis in the neighbourhood of the irregular points

$$\frac{\partial\tau(l_3+0)}{\partial l}\neq\frac{\partial\tau(l_3-0)}{\partial l}$$

gives the Eqs. (29) and (17). Thus, the above justifies the present approach.

We shall show the potential of this approach for the model "flexure" (Fig. 9). Let the geometrical form of an interface be described by the formula $z=1+\delta/\pi\arctan[\alpha(x-0.4)]$ where δ is the difference between the depths of the wings of the flexure. The wavefields are shown in Fig. 10 for $\delta=\lambda_P/4$, where $\lambda_P=0.06$ km. The top seismogram is for the sloping flexure $\alpha=5$, the middle one for $\alpha=50$, and the bottom one for the very steep flexure $\alpha=500$. It is clearly seen that, for the small curvature of the interface, the wavefield may be obtained by the ray method. If the curvature of the interface is around $\alpha=50$, some kind of caustic phenomenon occurs in the form of a local loss of intensity caused by interference (0.35–0.45 km). If the curvature of the interface is extremely large, $\alpha=500$, the wavefield coincides with the field for a fault with small throw. In this case there are two reflections from the wings of the fault and two edge waves. The interference of the edge waves forms the field, the character of which depends on the value of the parameter δ.

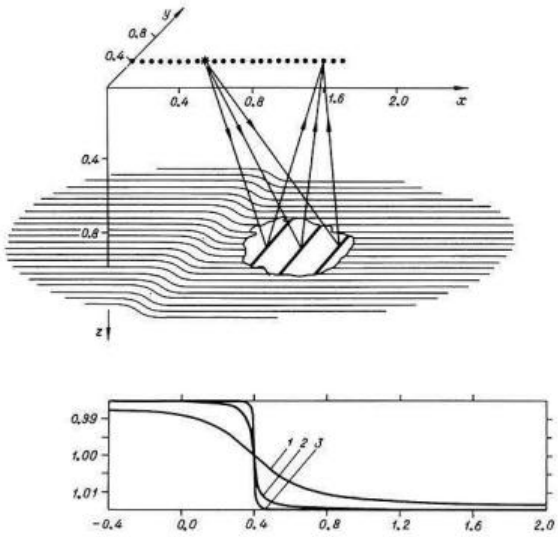

Fig. 9. Model of "flexure" (*top*) and its cross-section with the reflecting interfaces (*bottom*). Numbers corresponds to 1: $\alpha=5$, 2: $\alpha=50$, 3: $\alpha=500$. Edge rays, scattering from elements of the interface, are shown

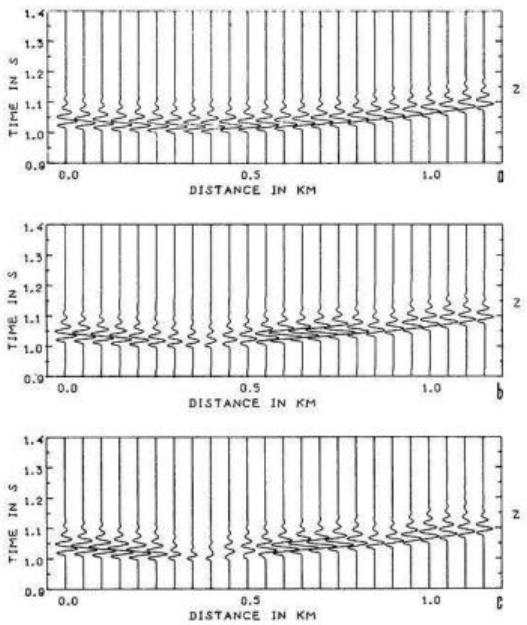

Fig. 10a–c. Theoretical seismograms for model of "flexure": **a** $\alpha=5$, **b** $\alpha=50$, **c** $\alpha=500$

Tip waves

The point of break (or the end) of a smooth edge is called *a tip*. The common tip of several edges is *a*

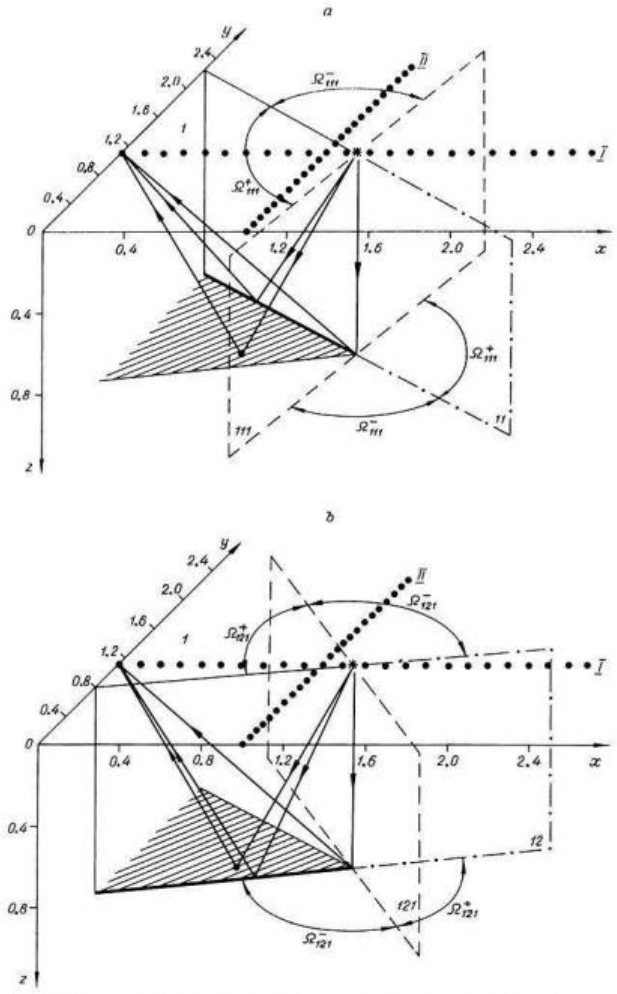

Fig. 11a and b. Model of "sector". Reflecting interface coincides with *shaded region*. Further explanation in text

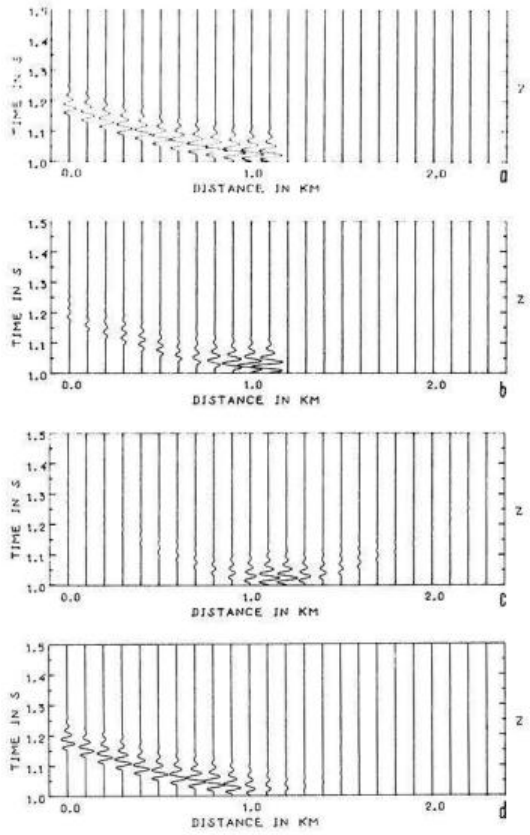

Fig. 12a–d. Theoretical seismograms for model of "sector" (profile I): **a** reflected wave, **b** edge waves (1.5 times enlarged), **c** tip waves (7.5 times enlarged), **d** total field

vertex. The sizes of edge wave domains are limited because of the tips. A single edge wave f_{mn} exists within the connected domain coinciding with the corresponding congruence of diffracted rays. This wavefield f_{mn} is continuous everywhere within its domain, with the exception of the primary shadow boundary, $\tau_{mn}=\tau_m$. This type of domain is called *the secondary illuminated zone* of the wave f_{mn}. A domain of absence of the wave ($f_{mn}\equiv 0$) is called *the secondary shadow zone*. A simply connected surface dividing the above zones is called *the secondary shadow boundary*. It looks like the surface of a curvilinear cone whose apex angle complies with the law of edge diffraction. Let mnp be the triple number of each secondary shadow boundary of the edge wave f_{mn}. The non-caustic shadow boundaries formed by tips are considered in the following.

Let us illustrate these definitions by an example of the reflection from an interface "sector". Its location is shown in Fig. 11. According to all the above, we have to describe the wavefield as a superposition of the reflected wave f_1 and two edge waves f_{11} and f_{12}. In Fig. 11 the primary shadow boundaries are marked by the indices 11 and 12 and the secondary shadow boundaries by the indices 111 and 121. The domain of existence of the reflected wave is marked by the index 1 and the domains of the secondary illuminated zones are located on the left of the dashed lines. Figures 12a and 13a show the reflected wave for two profiles marked by I and II. Figures 12b and 13b show the edge wavefields scattered from both edges.

One can see that a shortcoming of Eq. (17) appears as discontinuities of the wavefield f_{mn} at the secondary shadow boundaries. Let us see how this can be corrected.

Kinematics

Let us use a formal method to find the directions of rays arising from a tip. It concerns Snell's law in the form of Eq. (9). However, there are no limitations in choosing the directions of arising rays because the tip is not a linear element of interfaces. Any direction complies with the above-mentioned law formally. This fact is formulated as *the law of tip diffraction* (Keller, 1962). It reads as follows: the incident ray generates rays leaving the tip in all directions.

Let $\mathbf{e}_{mnp}$ be a unit vector of the tangent to a ray. Let this ray comply with the law of tip diffraction at that tip, which gives the mnp-th secondary shadow boundary. Then the differential equation

$$\frac{\mathrm{d}}{\mathrm{d}s}(\mathbf{e}_{mnp}/v_m)=\mathrm{grad}(1/v_m) \tag{31}$$

determines the congruence of *tip diffracted rays*.

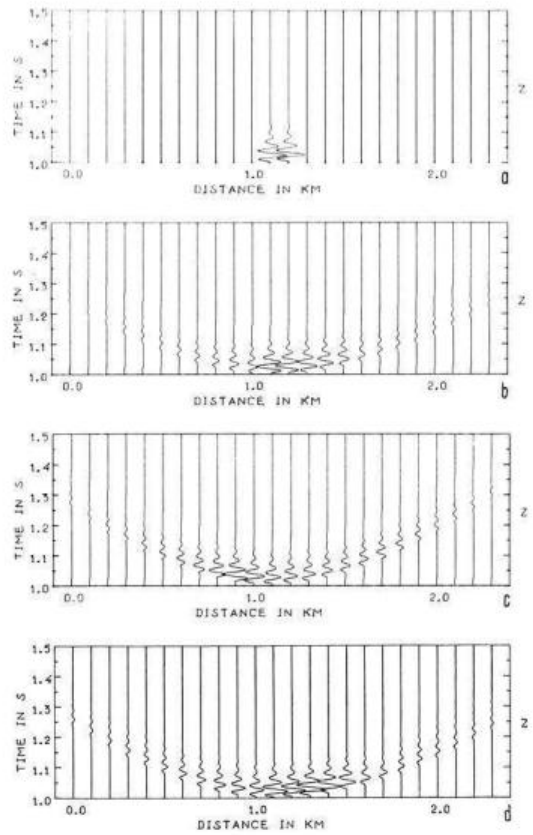

Fig. 13a–d. Theoretical seismograms for model of "sector" (profile II): **a** reflected wave (twice diminished), **b** edge waves (1.66 times diminished), **c** tip waves (4 times enlarged), **d** total field

A tip diffraction coefficient

Let a wave

$$f_{mnp}=\Phi_{mnp}\exp(i\omega\tau_{mnp}), \quad \operatorname{grad}\tau_{mnp}=\mathbf{e}_{mnp}/v_m \tag{32}$$

be connected with the mnp-th secondary shadow boundary. The latter may be given implicitly by the equation $\tau_{mnp}=\tau_{mn}$. The wave, Eq. (32), is called *a tip diffracted wave*. Let us divide the tip wave domain into separate parts. Suppose, the eikonal τ_{mn} may be continued analytically into the secondary shadow zone. The analytical continuation of the primary shadow boundaries $\tau_{11}=\tau_1$ and $\tau_{12}=\tau_1$ is shown in Fig. 11 by the dash-dotted lines.

Then the primary shadow boundary $\tau_{mn}=\tau_m$ and the secondary shadow boundary $\tau_{mnp}=\tau_{mn}$ divide the domain of the wave f_{mnp} into four parts. These parts are shown in Fig. 14. Let us give them the numbers 1, 2, 3 and 4, going around the line $\tau_{mnp}=\tau_{mn}=\tau_m$ clockwise or counter-clockwise, so that the shortest way from the fourth part to the first would coincide with the shortest way from the primary illuminated zone of the wave f_m to the primary shadow zone through the mn-th primary shadow boundary. The first and third parts have common points only at the line $\tau_{mnp}=\tau_{mn}=\tau_m$. The second and fourth parts have common points at the same line only. Let Ω^-_{mnp} be the symbol of the domain formed by the first and third parts. Let Ω^+_{mnp} be

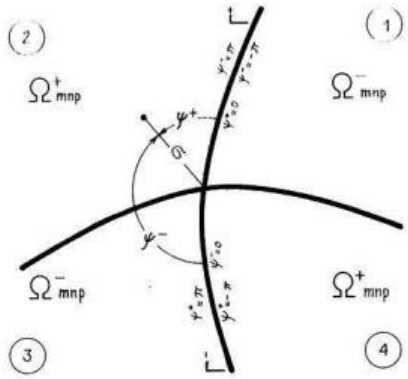

Fig. 14. The domains of continuity of a tip wave. Explanation in text

the symbol of the domain formed by the second and fourth parts. These domains in Fig. 11 for the secondary shadow boundary 111 are denoted by the symbols Ω^-_{111} and Ω^+_{111}. Let us denote the boundary between the first and second parts by Γ^+, and between the third and fourth parts by Γ^-. Γ^+ and Γ^- together form the secondary shadow boundary $\tau_{mnp}=\tau_{mn}$.

Let us represent the tip wave, Eq. (32), in the form:

$$f_{mnp}=f^+ + f^-, \quad f^\pm=\Phi^\pm\exp(i\omega\tau_{mnp}). \tag{33}$$

Let the sum $f_{mn}+f^+$ be continuous at the boundary Γ^+ and the sum $f_{mn}+f^-$ be continuous at the boundary Γ^-. Under the above conditions, we can find f^+ and f^- in the same way which is used for finding f_{mn}.

Let τ_{mnp}, $\psi^\pm$, σ be ray coordinates of the wave $f^\pm$. Here $\psi^\pm$ and σ give a congruence of the tip diffracted rays, i.e. every pair of fixed values $\psi^\pm=constant$ and $\sigma=constant$ gives a single ray. Let $\psi^\pm$ vary in the interval $-\pi\leqq\psi^\pm\leqq\pi$. We choose $\psi^\pm$ in such a way that the surface $\psi^\pm=0$ would coincide with the surface $\Gamma^\pm$, and the surfaces $\psi^\pm=\pi$ and $\psi^\pm=-\pi$ would coincide with $\Gamma^\mp$ (Fig. 14). Then

$$\begin{aligned}&\psi^\pm=\pm s_{mnp}|\psi^\pm| \quad \text{when } |\psi^\pm|<\pi/2,\\ &\psi^\pm=\pm s_{mnp}(|\psi^\pm|-\pi) \quad \text{when } |\psi^\pm|>\pi/2,\end{aligned} \tag{34}$$

$$\begin{aligned}&s_{mnp}=+1 \quad \text{within } \Omega^+_{mnp},\\ &s_{mnp}=-1 \quad \text{within } \Omega^-_{mnp}.\end{aligned} \tag{35}$$

Let us consider $\sigma=0$ at the line $\tau_{mnp}=\tau_{mn}=\tau_m$.

In the first place, let us take the case when the amplitude Φ_{mn} of the wave (11) is a scalar. Let the edge wavefield, Eq. (11), be a function of the above ray coordinates

$$f_{mn}=\Phi_{mn}(\tau_{mnp},\psi^\pm,\sigma)\exp[i\omega\tau_{mn}(\tau_{mnp},\psi^\pm,\sigma)]. \tag{36}$$

Then, in the neighbourhood of the secondary shadow boundary, this wavefield may be represented by the discontinuous function

$$\begin{aligned}&f_{mn}=f_{mn}(\tau_{mnp},\psi^\pm,\sigma) \quad \text{when } -\pi<\psi^\pm<0,\\ &f_{mn}=0 \quad \text{when } 0<\psi^\pm<\pi\end{aligned} \tag{37}$$

which displays explicitly the shortcoming of Eq. (17).

Figures 12a and 13a illustrate the discontinuity of the reflected wave. Figure 13b shows the change of sign of two edge waves at the primary shadow boundary 12 ($y=1.06$ km) and at the primary shadow boundary 11 ($y=1.25$ km). In Fig. 12b the discontinuity of the edge wave amplitudes is seen at the secondary shadow boundary $x=1.15$ km.

Suppose Eq. (37) represents an analytical function of the variable $\psi^{\pm}$ and allows us to make an analytical continuation into the complex plane of $\psi^{\pm}$ for any permissible values τ_{mnp} and σ. Let us find $\tilde{f}^{\pm}$ among the piecewise-analytical functions decreasing at infinity ($\tilde{f}^{\pm}\to 0$ when $|\psi^{\pm}|\to\infty$). Then we may construct the following integral of Cauchy's type

$$\tilde{f}^{\pm}=\frac{1}{2\pi i}\int_L f_{mn}(\tau_{mnp},\psi^{\pm}+\alpha,\sigma)\,\frac{\mathrm{d}\alpha}{\alpha}. \tag{38}$$

The specific type of the contour L will be given in the following. The properties of the similar integral, Eq. (14), have been discussed above. Equation (38) has a discontinuity at $\psi^{\pm}=0$. However, the superposition of Eqs. (37) and (38) is continuous at this point. The problem is that integral (38) has two extra discontinuities at $\psi^{\pm}=-\pi$ and $\psi^{\pm}=\pi$ because of the limited interval $-\pi\leqq\psi^{\pm}\leqq\pi$. To eliminate these discontinuities we take the periodic function of $\psi^{\pm}$, i.e.

$$f^{\pm}=\sum_{k=-\infty}^{\infty}\tilde{f}^{\pm}(\tau_{mnp},\psi^{\pm}+2\pi k,\sigma). \tag{39}$$

Inserting Eq. (38) into Eq. (39) and using the well-known formula

$$\sum_{k=-\infty}^{\infty}(z-2\pi k)^{-1}=1/2\cdot\cot(z/2) \tag{40}$$

we get:

$$f^{\pm}=\frac{1}{4\pi i}\int_L f_{mn}(\tau_{mnp},\psi^{\pm}+\alpha,\sigma)\cot(\alpha/2)\,\mathrm{d}\alpha. \tag{41}$$

Integral (41) has the following properties. It is zero when $|\psi^{\pm}|\to\infty$. It has a discontinuity at $\psi^{\pm}=0$. However, the superposition of Eqs. (37) and (41) is a continuous and analytical function of $\psi^{\pm}$ in the neighbourhood of the surface $\psi^{\pm}=0$. If function (37) is a solution of some linear differential equation (for example, the wave equation) within the domain $-\pi<\psi^{\pm}<0$, the superposition of Eqs. (37) and (41) complies with the same equation within the whole domain $-\pi\leqq\psi^{\pm}\leqq\pi$.

When $\omega\to\infty$, the asymptotic value of integral (41) is formed by contributions within a small neighbourhood of the saddle point $\alpha=-\psi^{\pm}$. Let us take the standard approximation at this point

$$\Phi_{mn}(\tau_{mnp},\psi^{\pm}+\alpha,\sigma)\approx\Phi_{mn}(\tau_{mnp},0,\sigma) \tag{42}$$

and for $|\sigma|\ll 1$ use the following relations

$$\tau_{mn}(\tau_{mnp},\psi^{\pm},\sigma)\approx\tau_{mnp}-A\sin^2\psi^{\pm},$$
$$A=\tau_{mnp}-\tau^{*}\approx\tau_{mnp}-\tau_m, \tag{43}$$
$$\tau^{*}=\tau_{mn}(\tau_{mnp},\psi^{\pm},\sigma)\quad\text{with}\quad|\psi^{\pm}|=\pi/2,$$
$$|\psi^{\pm}|=\arcsin\sqrt{(\tau_{mnp}-\tau_{mn})/(\tau_{mnp}-\tau_m)}. \tag{44}$$

Let us note that Eq. (43) may be derived by using a similar method as in the case $v_m=constant$ (Klem-Musatov, 1981a).

Let the contour L within a neighbourhood of the saddle point coincide with *the steepest descent path*

$$\mathrm{Im}[i\omega\tau_{mn}(\tau_{mnp},\psi^{\pm}+\alpha,\sigma)]=\mathrm{Im}[i\omega\tau_{mn}(\tau_{mnp},0,\sigma)],$$
$$\mathrm{Re}[i\omega\tau_{mn}(\tau_{mnp},\psi^{\pm}+\alpha,\sigma)]<0.$$

Using Eq. (43) gives the following equations for this part of the contour

$$\mathrm{Re}\,\alpha+\psi^{\pm}=-\mathrm{Im}\,\alpha\qquad\text{for }\tau_{mnp}>\tau_m,$$
$$\mathrm{Re}\,\alpha+\psi^{\pm}=\mathrm{Im}\,\alpha\qquad\text{for }\tau_{mnp}<\tau_m.$$

The integral exists if the contour approaches to the points $\mathrm{Im}\,\alpha=\pm\infty$ within domains

$$\mathrm{Re}[i\omega\tau_{mn}(\tau_{mnp},\psi^{\pm}+\alpha,\sigma)]<0.$$

Using Eq. (43) allows us to obtain this condition for $\mathrm{Im}\,\alpha\to\infty$ in the following form

$$-\pi/2<\mathrm{Re}\,\alpha+\psi^{\pm}<0\qquad\text{when }\tau_{mnp}>\tau_m,$$
$$0<\mathrm{Re}\,\alpha+\psi^{\pm}<\pi/2\qquad\text{when }\tau_{mnp}<\tau_m,$$

and for $\mathrm{Im}\,\alpha\to-\infty$ in the form

$$0<\mathrm{Re}\,\alpha+\psi^{\pm}<\pi/2\qquad\text{when }\tau_{mnp}>\tau_m,$$
$$-\pi/2<\mathrm{Re}\,\alpha+\psi^{\pm}<0\qquad\text{when }\tau_{mnp}<\tau_m.$$

The contours are shown in Fig. 5a for $\tau_{mnp}>\tau_m$ and in Fig. 5b for $\tau_{mnp}<\tau_m$ (in these figures, $q=2$ and term η must be replaced by $\psi^{\pm}$).
Then integral (41) may be written as

$$f^{\pm}=\Phi_{mn}(\tau_{mnp},0,\sigma)\,\Psi^{\pm}\exp(i\omega\tau_{mnp}),$$
$$\Psi^{\pm}=\frac{1}{4\pi i}\int_L\cot[(\alpha-\psi^{\pm})/2]\exp[i\omega(\tau_m-\tau_{mnp})\sin^2\alpha]\,\mathrm{d}\alpha. \tag{45}$$

To discuss the accuracy of this expression, we would repeat all that was said concerning Eq. (17). Equation (45) gives a satisfactory description within the so-called boundary layer where the amplitude of a tip wave changes rapidly. Within this domain the amplitude Φ_m may be considered as a function of the free point $\Phi_m(\tau_{mnp},\psi^{\pm},\sigma)$. The real accuracy of description is independent of the choice of the versions:

$$\Phi_m(\tau_{mnp},0,\sigma)\quad\text{or}\quad\Phi_m(\tau_{mnp},\psi^{\pm},\sigma).$$

Consideration of Eqs. (17), (34), (44), (45) and using identical mathematical transformations (for details, see Klem-Musatov, 1981a, b) allow us to write Eq. (33) in the form:

$$f_{mnp}=s_{mnp}\Phi_m H(\rho_{mnp},\zeta_{mnp})\exp(i\omega\tau_{mnp}), \tag{46}$$
$$H(\rho,\zeta)=W(\rho)\,\Psi(\rho,\zeta), \tag{47}$$

$$\Psi(\rho,\zeta)=\sin(2\zeta)/\pi\cdot\int_0^1[x^2-2x\cos(2\zeta)+1]^{-1}$$
$$\cdot\exp[i\pi\rho^2(x+x^{-1}-2)/8]\,dx,$$
$$\rho_{mnp}=\sqrt{2\omega(\tau_{mnp}-\tau_m)/\pi},$$
$$\zeta_{mnp}=\arcsin\sqrt{(\tau_{mnp}-\tau_{mn})/(\tau_{mnp}-\tau_m)}, \qquad (48)$$

where H may be regarded as *a tip diffraction coefficient*. If $\tau_{mnp}<\tau_m$, we have $\rho_{mnp}=ix$, $x=\sqrt{2\omega(\tau_m-\tau_{mnp})/\pi}$, $H(ix,\zeta)=\overline{H(x,\zeta)}$, where $\overline{H}$ denotes the complex conjugate of H. In these formulae we may use the analytical continuation of the amplitude Φ_m and the eikonals τ_m, τ_{mn} into the primary and secondary shadow zones by means of any type of parameterization of space.

Let us return to the example "sector" (Fig. 11). Now we can write the total wavefield in the form

$$f=f_1+\sum_{n=1}^{2}(f_{1n}+f_{1n1})$$

where f_{1n1} is a tip wave. Figures 12c and 13c show the tip waves computed by Eq. (46). It is possible to see in Fig. 13c the change of sign of their amplitudes at the secondary shadow boundaries 111 ($y=0.95$ km) and 121 ($y=1.66$ km). Figures 12d and 13d show the total wavefield formed by the interference of the reflected wave, two edge waves and two tip waves. The total field is regular everywhere.

If $0\leqq\rho<\infty$, $0\leqq\zeta\leqq\pi/2$, we have the following approximate formulae

$$\Psi(\rho,\zeta)=\Psi(0,\zeta)-i\rho^2\sin\zeta/8\cdot\ln(\pi\rho^2/8) \quad \text{when } \rho\to 0, \qquad (49)$$
$$\Psi(\rho,\zeta)=(\sqrt{2}\pi\rho)^{-1}(\zeta^{-1}-\cot\zeta)\exp(i5\pi/4)$$
$$+W(\rho\zeta)+O(\rho^{-2}) \quad \text{when } \rho\to\infty, \qquad (50)$$
$$\Psi(0,\zeta)=1/2-\zeta/\pi, \quad \Psi(\rho,0)=1/2, \quad \Psi(\rho,\pi/2)=0 \qquad (51)$$

where O is the symbol of asymptotic estimation. The point $\rho=0$ is the essential special point because the value of the function depends on the direction along which this point is approached. However, the total wavefield at this point is determined uniquely. Let us give the corresponding result.

Every single wavefield f_m has only two primary shadow boundaries within the small neighbourhood of the line $\tau_{mnp}=\tau_{mn}=\tau_m$, i.e. at $\rho=0$ (Fig. 15). Let us call their indices $n=a$ and $n=b$. Let γ_m be the dihedral angle between the tangent planes to the ma-th and mb-th primary shadow boundaries at a point of the line $\tau_{mnp}=\tau_{mn}=\tau_m$ with $n=a$ and $n=b$. This angle must be taken within (and not outside) the primary illuminated zone. Then at this point the following equality exists:

$$f_m+f_{ma}+f_{mb}+f_{map}+f_{mbp}=f_m\gamma_m/2\pi. \qquad (52)$$

Figure 16 shows the graphs of modulus and argument of the function (48).

Interrelation with known physical ideas

It was shown (Aizenberg, 1982) that Eq. (46) matches the classical theory of diffraction. If $v_m=constant$, the

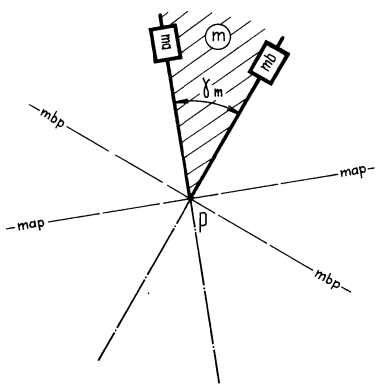

Fig. 15. The neighbourhood of a singular point of the primary illuminated zone (*shaded region*). Explanation in text

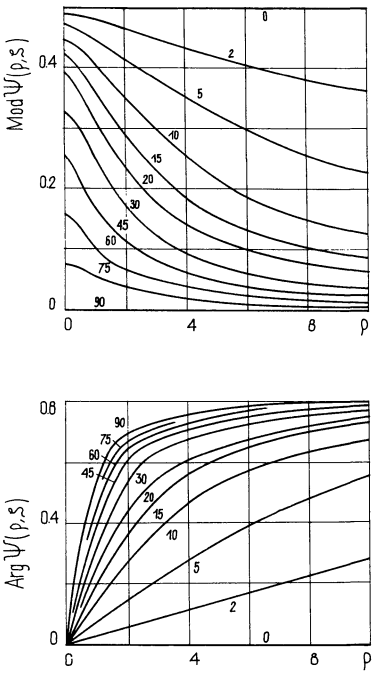

Fig. 16. Modulus and argument of function $\Psi(\rho,\zeta)$. Numbers at the curves give the values of ζ, expressed in degrees

tip wave can be found by asymptotic analysis of Kirchhoff's integral in the form of Eq. (46), where

$$H(\rho,\zeta)=\rho\cos\zeta/(2\pi)\int_{\rho\sin\zeta}^{\infty}(x^2+\rho^2\cos^2\zeta)^{-1}$$
$$\cdot\exp[i\pi(x^2-\rho^2\sin^2\zeta)/2]\,dx. \qquad (53)$$

It has been shown, both numerically and analytically, that this function is identical with the product in Eq. (47). It allows us to represent the superposition of Eqs. (17) and (46) in the form:

$$f_{mn}+f_{mnp}=f_mG(s_{mn}\sqrt{\pi/2}\,\rho\cos\zeta,s_{mnp}\sqrt{\pi/2}\,\rho\sin\zeta), \qquad (54)$$
$$G(a,b)=a/(2\pi)\cdot\int_b^{\infty}(x^2+a^2)^{-1}\exp[i(x^2+a^2)]\,dx, \qquad (55)$$

where $G(a,b)$ is the so-called generalized Fresnel integral (Clemmow and Senior, 1953) $\rho=\rho_{mnp}$, $\zeta=\zeta_{mnp}$.

Let us show with the simplest example that Eq. (46) complies with Fock's parabolic equation of *transverse two-dimensional diffusion* which describes diffusion of wave energy out of the secondary illuminated zone into the secondary shadow zone. Let the wave velocity be constant and wave f_m be plane ($\Phi_m = constant$) with its wave vector perpendicular to an edge containing a point of break. Let (R, θ, φ) be spherical coordinates, where R is the distance from the tip, θ is the angle between the tip ray and the ray $\theta = 0$ which coincides with the intersection of the primary and secondary shadow boundaries, φ is the angle between the mnp-th secondary shadow boundary $\varphi = 0$ and the plane which contains the given tip ray and the ray $\theta = 0$.

By substitution of Eq. (46) into Helmholtz's equation $(\Delta + k_m^2) f_{mnp} = 0$, where $k_m = \omega / v_m$, neglecting all values of order less than k_m and using a linear approximation for trigonometric functions of small argument, we can obtain the equation of transverse diffusion

$$\frac{2ik_m}{R}\frac{\partial}{\partial R}(R\Phi_{mnp}) + \frac{1}{R^2\theta}\frac{\partial}{\partial\theta}\Phi_{mnp} + \frac{1}{R^2}\frac{\partial^2}{\partial\theta^2}\Phi_{mnp} + \frac{1}{R^2\theta^2}\frac{\partial^2}{\partial\varphi^2}\Phi_{mnp} = 0. \tag{56}$$

Using the following relations in the neighbourhood of the ray $\theta = 0$

$$\rho_{mnp} = \sqrt{2\omega(\tau_{mnp} - \tau_m)/\pi} = \sqrt{2k_m R(1-\cos\theta)/\pi} \approx \theta\sqrt{k_m R/\pi},$$

$$\zeta_{mnp} = \arcsin\sqrt{(\tau_{mnp} - \tau_{mn})/(\tau_{mnp} - \tau_m)} = \arcsin\sqrt{[1-(\cos^2\theta + \sin^2\theta\cos^2\varphi)^{1/2}]/(1-\cos\theta)} \approx \varphi, \tag{57}$$

we can represent Eq. (56) in the form

$$2\pi i\rho^2\Phi_{mnp} + (\pi i\rho^3 + \rho)\frac{\partial}{\partial\rho}\Phi_{mnp} + \rho^2\frac{\partial^2}{\partial\rho^2}\Phi_{mnp} + \frac{\partial^2}{\partial\zeta^2}\Phi_{mnp} = 0. \tag{58}$$

The solution of this equation is $\Phi_{mnp} = H(\rho_{mnp}, \zeta_{mnp})$ where H is the integral (53). Thus, Eq. (46) describes a phenomenon of transverse diffusion in the form of the tip wave. Analysis shows the following mechanism of this phenomenon. The wave energy flows from the secondary illuminated zone through the secondary shadow boundary into the secondary shadow zone around the ray $\theta = 0$. Hence, unlike the diffusion mechanism described earlier, the tip wave is formed by a type of three-dimensional eddy diffusion around the ray $\theta = 0$.

Polarization

Now let us take the case where the amplitude of the wave (11) is the vector (25). Let us represent the tip wave (32) in the form:

$$f_{mnp} = \sum_{q=1}^{3} \mathbf{j}_q f_{mnp}^{(q)}, \qquad f_{mnp}^{(q)} = \varphi_{mnp}^{(q)} \exp(i\omega\tau_{mnp}) \tag{59}$$

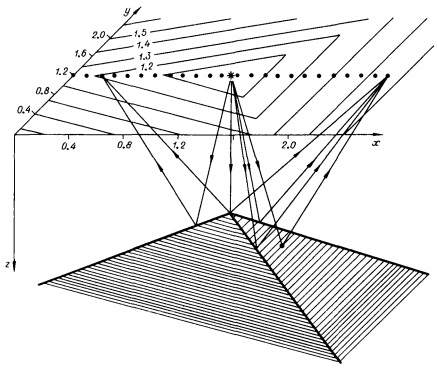

Fig. 17. Model of "pyramid". Reflecting interface is given by depth lines on the plane of observation

where $f_{mnp}^{(q)}$ are scalars. Let us use the same approach, Eqs. (33)–(46), for every function $\varphi_{mnp}^{(q)}(\tau_{mnp}, \psi^{\pm}, \sigma)$ which has been used for the scalar case. It allows us to determine three scalar functions

$$f_{mnp}^{(q)} = s_{mnp}\varphi_m^{(q)} H(\rho_{mnp}, \zeta_{mnp}) \exp(i\omega\tau_{mnp}) \quad \text{with} \quad q = 1, 2, 3. \tag{60}$$

Inserting Eq. (60) into Eq. (59) gives Eq. (46) again, where Φ_m is the vector (6).

This result may be interpreted in the same way as for the edge wave above. Let $\mathbf{p}_{mnp}$ be a unit vector of polarization of the tip wave f_{mnp}. In accordance with the general theory, this vector must coincide with $\mathbf{e}_{mnp}$ (for a longitudinal wave) or be perpendicular to $\mathbf{e}_{mnp}$ (for a transverse wave). However, in Eq. (46) the vector $\mathbf{p}_{mnp}$ coincides with $\mathbf{p}_m$. In fact, the real accuracy of description is independent of this discrepancy because the latter is of no importance within the boundary layer. The vector Φ_m may be considered as a function of a free point in space and continued analytically into the shadow zones.

The ray method including diffraction on edges and vertices

The present modification of the ray method results in the addition of edge, Eq. (17), and tip, Eq. (46), waves to the reflected/transmitted wavefield, Eq. (4),

$$f = \sum_m [f_m + \sum_n (f_{mn} + \sum_p f_{mnp})].$$

This approach can be used in any inhomogeneous media with piecewise-smooth edges of interfaces outside caustic zones. Here we shall show two simple examples of using this approach.

Let the interface by pyramid-shaped (Fig. 17). The total wavefield is given in the form

$$f = \sum_{m=1}^{3}\left[f_m + \sum_{n=1}^{2}(f_{mn} + f_{mn1})\right]$$

where m is the index of a face of the interface and f_{mn1} is a tip wave. Figure 18 shows the wavefield scattered by this interface. Note, that all six tip waves have the

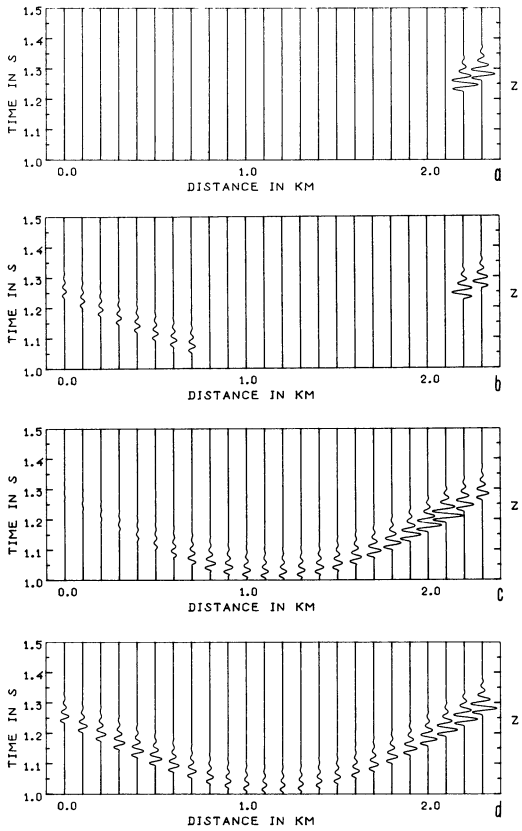

Fig. 18a–d. Theoretical seismograms for model of "pyramid": **a** reflected wave (twice diminished), **b** edge waves (twice diminished), **c** tip waves (1.5 times enlarged), **d** total field

same eikonal and form a common diffracted wave scattering from the vertex of the interface.

Let us next consider the model "faults". It is known that, in seismic prospecting and deep seismic sounding, the observed waves often have a complex group (multiphase) character inspite of a rather simple source signal shape. The simplest example of the formation of multiphase groups is obtained from an examination of reflections from a boundary disturbed by a system of faults with small throw.

Let the interface be disturbed by two intersecting systems of faults, where each system contains four parallel faults of infinite extension (Fig. 19). Unlike the previous examples, the elements of the interface differ in their number of edges and the edges differ in their number of tips. Let us mark the elements with four edges by $m=1, 2, \ldots, 9$, those with three edges by $m=10, 11, \ldots, 21$, and those with two edges by $m=22, 23, \ldots, 25$. Then the total wavefield may be written in the form

$$f = f^1 + f^2 + f^3,$$

$$f^1 = \sum_{m=1}^{9} \left[f_m + \sum_{n=1}^{4} \left(f_{mn} + \sum_{p=1}^{2} f_{mnp} \right) \right],$$

$$f^2 = \sum_{m=10}^{21} \left[f_m + \sum_{n=1}^{2} (f_{mn} + f_{mn1}) + f_{m3} + f_{m31} + f_{m32} \right],$$

$$f^3 = \sum_{m=22}^{25} \left[f_m + \sum_{n=1}^{2} (f_{mn} + f_{mn1}) \right].$$

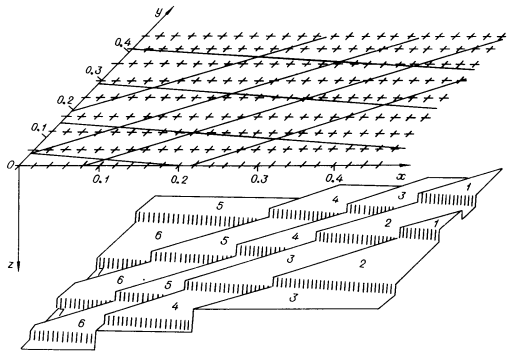

Fig. 19. Model of "faults". Projection of faults is given on the plane of observation. Further explanations in text

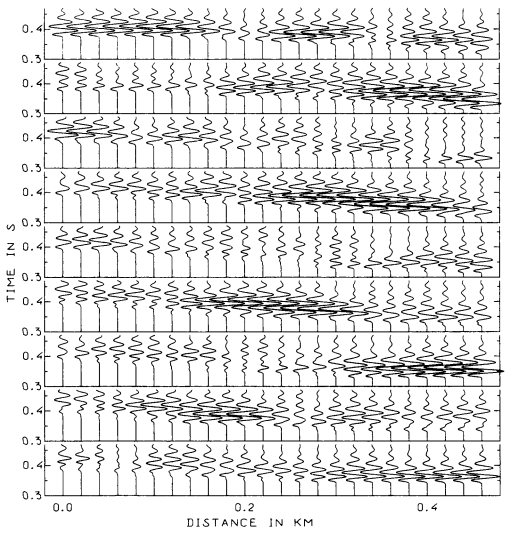

Fig. 20. Theoretical seismogram for model of "faults" ($h=5\lambda_P$)

Let the minimal distance of the interface from the plane of observation be $h=N\lambda_P$ where λ_P is the P wavelength. The depth of each block of interface is given by the formula $z=h+k\lambda_P/4$ where k is given in Fig. 19. Figures 20 and 21 show seismograms of the wavefield scattered by the disturbed interface for $h=5\lambda_P$ and $h=50\lambda_P$, respectively.

These examples show that for relatively small depth ($h=5\lambda_P$) the lineups mainly represent the block structure of the interface with characteristic horizontal dimensions of the blocks of 2–$3\lambda_P$ (and, obviously, larger). Under these conditions, the character of the wave patterns is determined by that part of the field which is controlled by the laws of geometrical seismics (ray transport of energy). The diffraction components (mechanism of transverse diffusion) have a subordinate character, smoothing the characteristics of the field and complicating it by interference effects. With increasing depth of the interface, the role of diffraction components increases since the absolute dimensions of the zones of influence of diffusion mechanisms – the vicinity of the reflection point – increase. For relatively great depth ($h=50\lambda_P$), the diffusion mechanism plays the dominant role in the formation of fields from disturbed interfaces. Interference of diffraction components

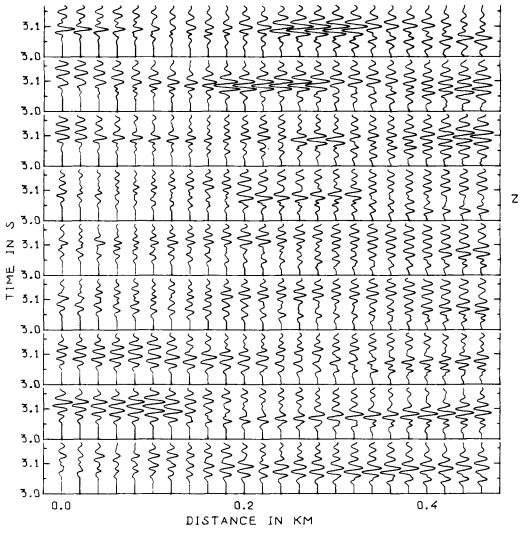

Fig. 21. Theoretical seismogram for model of "faults" ($h = 50\,\lambda_P$)

generates multiphase trains, the character of which depends on the degree of disturbance of the interface.

The method of superposition of tip waves

Equations (4), (17) and (46) allow us to compute wavefields in 3-D inhomogeneous media with piecewise-smooth edges of interfaces outside caustic zones. There is an approach, based on the above formulae, which can be used within caustic zones as formed by the curvature of interfaces. Its idea is a generalization of the approach described in an earlier section.

According to the present approach, the wavefield scattered by a rectifiable interface can be replaced approximately by the field scattered by a piecewise-plane boundary, approximating it with a sufficiently large number of plane elements. But, unlike the method described earlier, it can be done by means of triangulation. In the first place, the interface must be divided into regular parts so that some regular surface curvilinear coordinates (ξ, η) can be introduced in each of them. Each regular part can be divided into a set of curvilinear tetragons by cutting out along both coordinate lines. Each tetragon can be divided into two triangular elements. Thus the element of the approximating boundary is the plane triangle. This approximation guarantees finite values of the term Φ_m in Eqs. (4) and (46) because these terms do not now depend on the curvature of the initial interface. The wavefield scattered by the piecewise-plane boundary is a superposition of fields scattered by the plane elements composing it.

For a sufficiently small step of approximation the contributions from the elements, containing reflection/transmission points and points of edge diffraction, are small enough and may be neglected. Then the field scattered by the individual plane element will be a superposition of six tip waves diverging from its tips. The total field can be represented by superposition of just tip waves alone:

$$f = \sum_{m=1}^{M} \Delta f_m, \qquad \Delta f_m = \sum_{n=1}^{3} \sum_{p=1}^{2} f_{mnp}, \qquad m \neq m_0,\ n \neq n_0 \quad (61)$$

where m is the index of an element, n – the index of an edge of the m-th element, p – the index of a tip of the mn-th edge, m_0 and n_0 are the indices of the elements containing the corresponding reflection/transmission points and the points of edge diffraction. Every term Δf_m of this sum is strictly bounded. That is why the sum in Eq. (61) is limited within caustic zones caused by the curvature of the initial interface.

To justify the above approach we take Eq. (61) to the limit of the initial interface, simultaneously letting the step of approximation tend to zero and increasing the number of elements. In this case

$$\lim_{\substack{\max\{\Delta S_m\} \to 0 \\ M \to \infty}} \sum_{m=1}^{M} \Delta S_m = \iint_S \mathrm{d}S,$$

$$f = \iint_S F(\xi, \eta) \exp[i\omega\tau(\xi, \eta)]\, \mathrm{d}\xi\, \mathrm{d}\eta, \quad (62)$$

$$F(\xi, \eta) = \Phi_0(\xi, \eta)[-i\omega/(4\pi)]\left[\sqrt{(\tau_\xi - \tau_0)/(\tau - \tau_\xi)} + \sqrt{(\tau_\eta - \tau_0)/(\tau - \tau_\eta)}\right] \left|\frac{\partial\tau}{\partial\xi} \cdot \frac{\partial\tau}{\partial\eta}\right| (\tau - \tau_0)^{-1},$$

where $\Phi_0(\xi, \eta)$ and τ_0 are the amplitude and the eikonal of the analytical reflection/transmission for point (ξ, η), τ_ξ and τ_η are the eikonals of the analytical edge diffraction. Here the analytical edge diffraction stands for the diffraction by the rectilinear edge which is tangent to the coordinate line $\xi = constant$ or $\eta = constant$ for point (ξ, η).

Equation (62) can be regarded as a new asymptotic formulation of *the concept of secondary sources*. According to this formulation the value of the field at any point of the medium will be the superposition of secondary waves with amplitude $F(\xi, \eta)\,\mathrm{d}\xi\,\mathrm{d}\eta$ diverging from each point of the initial interface. Unlike the Fresnel and Kirchhoff descriptions, the amplitudes of the secondary waves in Eq. (62) are strictly bounded on the surface of integration.

The asymptotic analysis in the neighbourhood of the isolated stationary point of the first order (ξ_1, η_1) gives the wavefield (62) in the form of a regular wave

$$f = \Phi(\xi_1, \eta_1) \exp[i\omega\tau(\xi_1, \eta_1)],$$

$$\Phi(\xi_1, \eta_1) = F(\xi_1, \eta_1)/(i\omega h^{1/2}),$$

$$h = \frac{\partial^2\tau(\xi_1, \eta_1)}{\partial\xi^2} \cdot \frac{\partial^2\tau(\xi_1, \eta_1)}{\partial\eta^2} - \left[\frac{\partial^2\tau(\xi_1, \eta_1)}{\partial\xi\,\partial\eta}\right]^2. \quad (63)$$

If the wave velocity is constant this formula coincides with the formula of the ray method. This justifies the present approach.

We illustrate this approach for the model "syncline" (Fig. 22). Its geometrical shape is given by the equation

$$z = 1 + 0.1 \exp[-32(x - 1.15)^2 - 128(y - 1.15)^2].$$

Figure 23 shows the wavefield scattered by this interface. It is seen that the typical "loop" structure of the wavefield occurs.

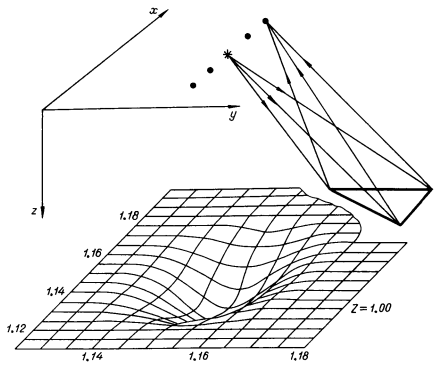

Fig. 22. Model of "syncline". Tip rays, scattering from an element of the interface, are shown. Further explanations in text

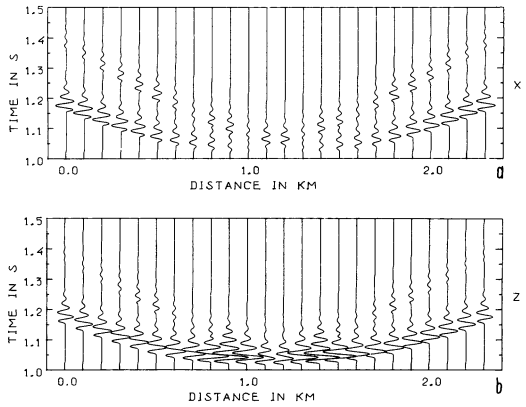

Fig. 23a and b. Theoretical seismograms for model of "syncline": **a** X-component (twice enlarged), **b** Z-component

Remarks

In conclusion, let us mention that there are many examples of mathematical modelling of wavefields in typical structures by the above method. There are theoretical seismograms for several types of pinch-out and low-amplitude faults (Klem-Musatov, 1980), interfaces of complex forms (Aizenberg and Klem-Musatov, 1980) and 3-D systems of intersecting faults (Klem-Musatov et al., 1982). The main principles of the generalization of the above approach for multiple diffraction are described in Klem-Musatov and Aizenberg (1984).

Acknowledgements. We wish to thank Prof. N.N. Puzyrev, who was the initiator of this study. Special thanks are due to our colleagues V.G. Chernyakov, who made the theoretical seismograms for model "pinch-out", and G.A. Klem-Musatova, who took a great part in writing computer programs and in seismic modelling. We are grateful to Professors A.S. Alekseyev, V.M. Babich, V. Červený and Dr. S.V. Goldin for useful discussions when this study was still in progress. We wish to thank Dr. P. Hubral, who invited us to submit the paper for publication.

Note added in proof. The secondary boundaries position in Fig. 11 is shown rough. Planes 111 and 121 must intersect profile II at the points $y=0.95$ km and $y=1.66$ km, respectively.

References

Aizenberg, A.M.: Scattering of seismic waves by broken edge of a flat boundary. Soviet Geol. and Geophys. **23**, 74–82, 1982

Aizenberg, A.M., Klem-Musatov, K.D.: Calculation of wave fields by the method of superposition of the edge waves. Soviet Geol. and Geophys. **21**, 79–94, 1980

Babich, V.M., Alekseyev, A.S.: A ray method of computing wave front intensities. Bull. Acad. Sci. USSR, Geophys. Ser. **1**, 9–15, 1958

Babich, V.M., Buldyrev, V.S.: Asymptotic methods in problems of diffraction of short waves (in Russian). Moscow: Nauka 1972

Born, M., Wolf, E.: Principles of optics. Oxford: Pergamon Press 1968

Červený, V.: Synthetic body wave seismograms for laterally varying layerd structures by the Gaussian beam method. Geophys. J.R. Astron. Soc. **73**, 389–426, 1983

Červený, V., Molotkov, I.A., Psenčík, I.: Ray method in seismology. Praha: Universita Karlova 1977

Claerbout, J.F.: Fundamentals of geophysical data processing. New York: McGraw-Hill 1976

Clemmow, P.S., Senior, T.B.A.: A note on generalized Fresnel integral. Proc. Camb. Phil. Soc. **9**, 570–572, 1953

Felsen, L.B., Marcuvitz, N.: Radiation and scattering of waves. New Jersey: Prentice-Hall, Englewood Clifts 1973

Fertig, J., Müller, G.: Approximate diffraction theory for transparent half-planes with application to seismic-wave diffraction at coal seams. J. Geophys. **46**, 349–367, 1979

Fock, V.A.: Electromagnetic diffraction and propagation problems. New York: Pergamon Press 1965

Hilterman, F.J.: Interpretative lessons from three-dimensional modelling. Geophysics **47**, 784–808, 1982

Karal, F.C., Keller, J.B.: Elastic wave propagation in homogeneous and inhomogeneous media. J. Acoust. Soc. Am. **31**, 694–705, 1959

Keller, J.B.: A geometrical theory of diffraction. J. Opt. Soc. Am. **52**, 116–130, 1962

Kennett, B.L.N.: Reflection operator methods for elastic waves. I – Irregular interfaces and regions. Wave Motion 1984 (in press)

Klem-Musatov, K.D.: The theory of edge waves and its applications in seismology (in Russian). Novosibirsk: Nauka 1980

Klem-Musatov, K.D.: Scattering of waves of a point fracture of a diffracting edge. Soviet Geol. and Geophys. **22**, 118–127, 1981a

Klem-Musatov, K.D.: Asymptotic formulae for the amplitude of wave scattered by a salient point on a diffracting edge. Soviet Geol. and Geophys. **22**, 108–114, 1981b

Klem-Musatov, K.D., Aizenberg, A.M.: Ray method and the theory of edge waves. Geophys. J.R. Astron. Soc. **79**, 35–50, 1984

Klem-Musatov, K.D., Aizenberg, A.M., Klem-Musatova, G.A.: An algorithm for mathematical modelling of three-dimensional diffraction fields. Soviet Geol. and Geophys. **23**, 116–121, 1982

Popov, M.M.: A new method of computations of wave fields in high-frequency approximation. Report LOMI AN SSSR, E-I-8I Leningrad, 1981

Trorey, A.W.: Diffraction for arbitrary source-receiver locations. Geophysics **42**, 1177–1182, 1977

Received August 28, 1984; Revised version February 28, 1985
Accepted March 20, 1985